Analytical solution for stability analysis of joined cross-ply thin laminated conical shells under axial compression

M. Shakouri*

Department of Aerospace Engineering, Semnan University, P.O. Box 35131-19111, Semnan, Iran

Abstract. The present research considers the stability and corresponding modes of two axially compressed joined cross-ply laminated conical shells. The joined conical shells are the general case of a wide area of joined structures, including cylinder-cone, cone-plate, cylinder-plate, stepped thickness cone and stepped thickness cylinder. The principle of minimum potential energy is applied to extract the equilibrium equations under the thin Donnell type shell theory assumptions. The analytical procedure is used to solve the equations by applying trigonometric and series responses in circumferential and meridional directions, respectively. To ensure from accuracy and correctness of the results, the finite element analysis is done for various stacking sequences and the analytical results are compared and validated with other literature and finite element results. Finally, the effects of some parameters including semi-vertex angles, meridional lengths, number of layers and various kinds of simply supported and clamped boundary conditions at both ends are studied.

Keywords: joined conical shells; cross-ply laminate; buckling; analytical solution

1. Introduction

Due to high capacity of load carrying, shells of revolution and joined shells find extensive uses in engineering branches like construction, mechanical and aeronautical structures. The joined shell structures, made from shell parts joined along their boundaries, experience high values of bending moment and shear force near the joining region. It causes the more instability in these structures. Therefore, the instability of the shells is one of the most important modes of failure of joined shell structures and needs more attention.

The stability and vibrational behavior of joined shells are one of the attractive subjects in recent years. Most previous investigations are focused on vibration of the joined shells (Shakouri and Kouchakzadeh 2014, Sarkheil *et al.* 2017, Bagheri *et al.* 2018, Izadi *et al.* 2018). However, there are some published papers on stability of joined shells. Flores and Godoy (1991) applied finite element analysis to study the buckling and post-buckling of cone-cylinder and sphere-cylinder shells under external pressure. A comprehensive review of recent works on joined shells is performed by Pietraszkiewicz and Konopinska (2015).

The elastic buckling and post-buckling of joined conical-cylindrical shells subjected to internal

---

*Corresponding author, Assistant Professor, E-mail: shakouri@semnan.ac.ir

pressure was studied by Teng and his colleagues (Teng 1996, Teng and Barbagallo 1997, Teng and Ma 1999, Zhao and Teng 2003), and the plastic buckling analysis of thick isotropic cone-cylinder and cap-cylinder shells for radius/thickness ratio of 50, under external pressure is investigated by Bushnel and Galletly (1974). Zerin (2012) studied the effect of non-homogeneity on the stability of laminated orthotropic conical shells subjected to hydrostatic pressure.

Anwen (1998) showed that the insertion of a toroidal segment between the cone and cylinder results in slightly higher external buckling pressures than that of cone–cylinder shell without transition. The nonlinear thermo-elastic buckling and post-buckling characteristics of laminated conical-cylindrical and conical–cylindrical–conical joined shells, subjected to uniform temperature rise is studied by Patel and his colleagues (Patel *et al*. 2005, 2006, 2008). Shakouri *et al*. (2016) investigated the buckling of conical shells under compression with various imperfection shapes.

The joined conical shells are a general case for a wide range of joined shells and plates. As an example, the joined cone-cylinder or joined cone-plate analyses are the special cases of two joined conical shells, when the semi-vertex angle tends to $0°$ or $90°$, respectively. Therefore, study of two joined conical shells can cover the results for the special cases mentioned above (Kouchakzadeh and Shakouri 2014). There are a few published papers on buckling of joined conical shells. The axisymmetric buckling of joined isotropic conical shells is studied in (Kouchakzadeh and Shakouri 2015) and a closed form solution is introduced. The stability of joined isotropic conical shells under axial compression is studied in (Shakouri and Kouchakzadeh 2013) for simply-supported boundary conditions at both ends.

As can be seen above, most of the previous works on the stability of joined shells are focused on isotropic materials and the buckling analysis of joined laminated conical shells need more attention. In this study, the buckling load and modes of two joined cross-ply conical shells under axial compression are studied. The governing equations and continuity conditions at joining section are obtained using minimum potential energy. The equations are solved by assuming trigonometric response in circumferential and series solution in meridional direction. The results are compared and validated with the available results in the other papers. Effects of semi-vertex angles, meridional lengths, number of layers and various boundary conditions on the buckling load are investigated.
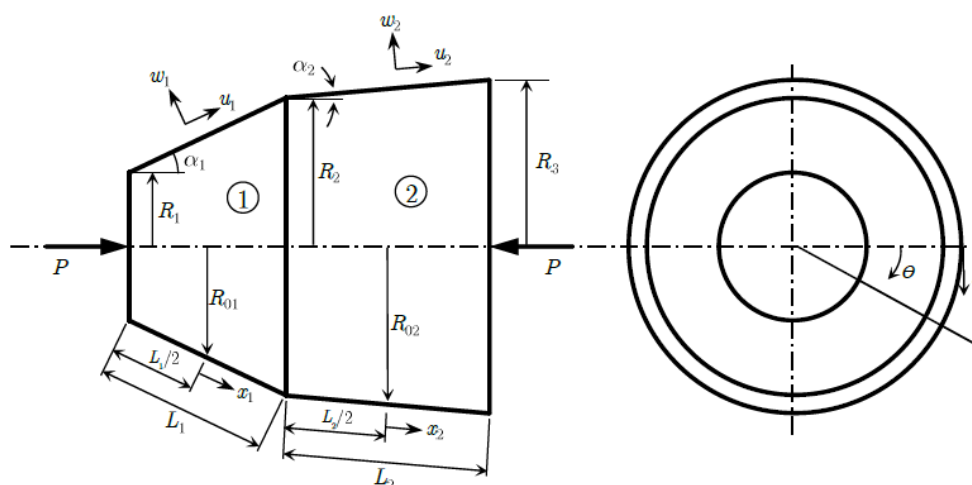
Fig. 1 Geometry of two joined conical shells
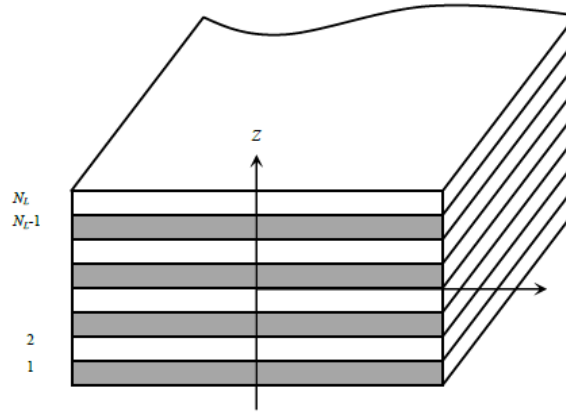
Fig. 2 Lamination of cross-ply layers

2. Governing equations for joined conical shells

2.1 Displacements and strains

Consider a set of two joined conical shells with (x,θ,z) coordinates as shown in Fig. 1, where x is the coordinate along the cones' generators with the origin placed at the middle of the generators, θ is the circumferential coordinate and z is the coordinate normal to the cones' surfaces as shown in Fig. 2. R_1, R_2 and R_3 are the radii of the system of cones at its first, middle and end, respectively, α_1 and α_2 the semi-vertex angles of cones and L_1 and L_2 are the cone lengths along the generators. The thicknesses of cones are t_1 and t_2.

The shells are made of N_L layers of laminates with the fibers in 0 or 90 degrees with respect to the x axis and the stacking sequences of the layers is as shown in Fig. 2.

Applying the classical shell theory, the displacement field is:

$$\bar{u}(x,\theta,z) = u(x,\theta) + z\beta_x(x,\theta)$$
$$\bar{v}(x,\theta,z) = v(x,\theta) + z\beta_\theta(x,\theta) \qquad (1)$$
$$\bar{w}(x,\theta,z) = w(x,\theta)$$

where the parameters $\bar{u}$, $\bar{v}$ and $\bar{w}$ are displacements, u, v and w are displacements of the mid-plane in x, θ and z directions respectively, and β_x and β_θ are rotations about x and θ directions, respectively.

According to the thin-walled shallow shell theory of Donnell-type, the strains and curvature changes in the middle surface of each cone can be written as (Qatu 2004)

$$\{\varepsilon\} = \left\{ \begin{array}{c} \varepsilon_x \\ \varepsilon_\theta \\ \gamma_{x\theta} \end{array} \right\} = \left\{ \begin{array}{c} \dfrac{\partial u}{\partial x} \\ \dfrac{1}{R(x)}(\dfrac{\partial v}{\partial \theta} + u\sin\alpha + w\cos\alpha) \\ \dfrac{1}{R(x)}\dfrac{\partial u}{\partial \theta} - \dfrac{1}{R(x)}v\sin\alpha + \dfrac{\partial v}{\partial x} \end{array} \right\} \qquad (2)$$

$$\{\kappa\} = \begin{Bmatrix} \kappa_x \\ \kappa_\theta \\ \kappa_{x\theta} \end{Bmatrix} = \begin{Bmatrix} \dfrac{\partial \beta_x}{\partial x} \\ \dfrac{1}{R(x)}(\beta_x \sin\alpha + \dfrac{\partial \beta_\theta}{\partial \theta}) \\ \dfrac{1}{R(x)}\dfrac{\partial \beta_x}{\partial \theta} + \dfrac{\partial \beta_\theta}{\partial x} - \dfrac{1}{R(x)}\beta_\theta \sin\alpha \end{Bmatrix} \tag{3}$$

where $R(x)$ is cone's radius at any point along its length and may be expressed as

$$R(x) = R_0 + x\sin\alpha \qquad -L/2 \le x \le L/2 \tag{4}$$

and

$$\beta_x = -\frac{\partial w}{\partial x} \qquad , \qquad \beta_\theta = -\frac{1}{R}\frac{\partial w}{\partial \theta} \tag{5}$$

The parameters ($\varepsilon_x, \varepsilon_\theta, \gamma_{x\theta}$) are the membrane strains, and ($\kappa_x, \kappa_\theta, \kappa_{x\theta}$) are the flexural (bending) strains, known as the curvatures.

2.2 Constitutive relations

The stress-strain relation for cross-ply laminated conical shell can be shown as (Reddy 2004)

$$\begin{Bmatrix} N_{xx} \\ N_{\theta\theta} \\ N_{x\theta} \\ M_{xx} \\ M_{\theta\theta} \\ M_{x\theta} \end{Bmatrix} = \begin{bmatrix} A_{11} & A_{12} & 0 & B_{11} & B_{12} & 0 \\ A_{12} & A_{22} & 0 & B_{12} & B_{22} & 0 \\ 0 & 0 & A_{66} & 0 & 0 & B_{66} \\ B_{11} & B_{12} & 0 & D_{11} & D_{12} & 0 \\ B_{12} & B_{22} & 0 & D_{12} & D_{22} & 0 \\ 0 & 0 & B_{66} & 0 & 0 & D_{66} \end{bmatrix} \begin{Bmatrix} \varepsilon_{xx} \\ \varepsilon_{\theta\theta} \\ \gamma_{x\theta} \\ \kappa_{xx} \\ \kappa_{\theta\theta} \\ \kappa_{x\theta} \end{Bmatrix} \tag{6}$$

in which (N_{xx}, $N_{\theta\theta}$, $N_{x\theta}$) and (M_{xx}, $M_{\theta\theta}$, $M_{x\theta}$) are stress and moment resultants measured per unit length, respectively and (A_{ij}, D_{ij}, B_{ij}) are extensional, bending and bending-extensional coupling stiffnesses which are defined in terms of the lamina stiffnesses Q_{ij} as

$$A_{ij} = \sum_{k=1}^{N_L} (\bar{Q}_{ij})_k (z_{k+1} - z_k) \qquad (i,j = 1,2,6)$$

$$B_{ij} = \frac{1}{2}\sum_{k=1}^{N_L} (\bar{Q}_{ij})_k (z_{k+1}^2 - z_k^2) \qquad (i,j = 1,2,6) \tag{7}$$

$$D_{ij} = \frac{1}{3}\sum_{k=1}^{N_L} (\bar{Q}_{ij})_k (z_{k+1}^3 - z_k^3) \qquad (i,j = 1,2,6)$$

where N_L is total number of layers in lamina, the subscript k denotes the kth layer of the laminate and $\bar{Q}_{ij}$s are transformed stiffnesses and for cross-ply laminates are expressed as

$$\overline{Q}_{11} = Q_{11}\cos^4\varphi + Q_{22}\sin^4\varphi$$
$$\overline{Q}_{12} = Q_{12}(\sin^4\varphi + \cos^4\varphi)$$
$$\overline{Q}_{22} = Q_{11}\sin^4\varphi + Q_{22}\cos^4\varphi \qquad \varphi = 0° \text{ or } 90°$$
$$\overline{Q}_{16} = 0 \tag{8}$$
$$\overline{Q}_{26} = 0$$
$$\overline{Q}_{66} = Q_{66}(\sin^4\varphi + \cos^4\varphi)$$

where φ is the angle of each ply and Q_{ij}s are known in terms of the engineering constants:

$$Q_{11} = \frac{E_1}{1 - v_{12}v_{21}}, \qquad Q_{12} = \frac{v_{12}E_2}{1 - v_{12}v_{21}}, \qquad Q_{22} = \frac{E_2}{1 - v_{12}v_{21}}, \qquad Q_{66} = G_{12} \tag{9}$$

2.3 Governing equations

The strain field can be used to drive the governing equations of isotropic conical shells by the use of minimum potential energy theory. We have

$$\delta\Pi = \delta(U - W) = 0 \tag{10}$$

where δU denotes the virtual strain energy, and δW is the virtual potential energy due to the applied loads.

$$\delta U = \int_V \sigma_{ij}\delta\varepsilon_{ij}\,dV = \int_\Omega \int_{-t/2}^{t/2} \sigma_{ij}\delta\varepsilon_{ij}R\,dx\,d\theta\,dz$$
$$= \int_\Omega [N_x\delta\varepsilon_x + M_x\delta\kappa_x + N_\theta\delta\varepsilon_\theta + M_\theta\delta\kappa_\theta + N_{x\theta}\delta\varepsilon_{x\theta} + M_{x\theta}\delta\kappa_{x\theta}]R\,dx\,d\theta \tag{11}$$

$$\delta W = \int_\Gamma [\hat{N}_x\delta u + \hat{T}_x\delta v + \hat{S}_s\delta w + \hat{M}_x\delta(\frac{\partial w}{\partial x})]R\,d\theta \tag{12}$$

Here, V is the volume of the shell, $\widehat{N_x}$, $\widehat{T_x}$, $\widehat{S_x}$, $\widehat{M_x}$ are stress resultants due to applied axial load, and (N, M) are stress resultants measured per unit length and defined as

$$\begin{bmatrix} N_x \\ N_\theta \\ N_{x\theta} \\ M_x \\ M_\theta \\ M_{x\theta} \end{bmatrix} = \int_{-t/2}^{t/2} \begin{bmatrix} \sigma_x \\ \sigma_\theta \\ \sigma_{x\theta} \\ z\,\sigma_x \\ z\,\sigma_\theta \\ z\,\sigma_{x\theta} \end{bmatrix} dz \tag{13}$$

By substitution of Eqs. (2)-(5) and Eq. (13) into Eqs. (11) and (12), we have

$$\delta U = \int_{\Omega} [(\frac{\partial(RN_x)}{\partial x} - N_\theta \sin\alpha + \frac{\partial N_{x\theta}}{\partial \theta})\delta u$$

$$+(\frac{\partial N_\theta}{\partial \theta} + \frac{1}{R}\frac{\partial M_\theta}{\partial \theta}\cos\alpha - \frac{\partial(RN_{x\theta} - M_{x\theta}\cos\alpha)}{\partial x}$$

$$-N_{x\theta}\sin\alpha + \frac{1}{R}M_{x\theta}\sin 2\alpha)\delta v + (\frac{\partial}{\partial x}(RN_x\frac{\partial w}{\partial x}) + \frac{\partial^2(RM_x)}{\partial x^2}$$

$$-N_\theta \cos\alpha + \frac{1}{R}\frac{\partial}{\partial\theta}(N_\theta\frac{\partial w}{\partial\theta}) - \frac{\partial M_\theta}{\partial x}\sin\alpha + \frac{1}{R}\frac{\partial^2 M_\theta}{\partial\theta^2} \quad\quad (14)$$

$$\frac{\partial}{\partial x}(N_{x\theta}\frac{\partial w}{\partial\theta}) + \frac{\partial}{\partial\theta}(N_{x\theta}\frac{\partial w}{\partial x}) + 2\frac{\partial^2 M_{x\theta}}{\partial x\partial\theta} + \frac{2}{R}\frac{\partial M_{x\theta}}{\partial\theta}\sin\alpha)\delta w]\,dx\,d\theta$$

$$+\int_{\Gamma} [(RN_x)\delta u - (RN_{x\theta} - M_{x\theta}\cos\alpha)\delta v + (RM_x)\delta(\frac{\partial w}{\partial x})$$

$$+(RN_x\frac{\partial w}{\partial x} + \frac{\partial(RM_x)}{\partial x} - M_\theta\sin\alpha + 2\frac{\partial M_{x\theta}}{\partial\theta} + N_{x\theta}\frac{\partial w}{\partial\theta})\delta w]\,d\theta$$

$$\delta W = \int_{\Gamma} [\hat{N}_x\delta u + \hat{T}_x\delta v + \hat{M}_x\delta(\frac{\partial w}{\partial x}) + \hat{V}_x\delta w]R\,d\theta \quad\quad (15)$$

Substituting δU and δW from Eqs. (14) and (15) into the virtual work statement (10), we obtain

$$\delta u : \frac{\partial N_x}{\partial x} + \frac{1}{R}(N_x - N_\theta)\sin\alpha + \frac{1}{R}\frac{\partial N_{x\theta}}{\partial\theta} = 0$$

$$\delta v : \frac{1}{R}\frac{\partial N_\theta}{\partial\theta} - \frac{\partial N_{x\theta}}{\partial x} - \frac{2}{R}N_{x\theta}\sin\alpha + \frac{1}{R}Q_\theta\cos\alpha = 0 \quad\quad (16)$$

$$\delta w : -\frac{1}{R}N_\theta\cos\alpha + \frac{\partial Q_x}{\partial x} + \frac{Q_x\sin\alpha}{R} + \frac{1}{R}\frac{\partial Q_\theta}{\partial\theta} + P.B.T. = 0$$

where Q_x and Q_θ denote the shear resultants at x and θ directions, respectively and are defined as

$$Q_x = \frac{\partial M_x}{\partial x} + \frac{1}{R}(M_x - M_\theta)\sin\alpha + \frac{1}{R}\frac{\partial M_{x\theta}}{\partial\theta}$$

$$Q_\theta = \frac{\partial M_{x\theta}}{\partial s} + \frac{1}{R}\frac{\partial M_\theta}{\partial\theta} + \frac{2}{R}M_{x\theta}\sin\alpha \quad\quad (17)$$

Also, *P.B.T.* is pre-buckling loads defined as

$$P.B.T. = \frac{1}{R}\left[\frac{\partial}{\partial x}(RN_{x0}\frac{\partial w}{\partial s} + N_{x\theta 0}\frac{\partial w}{\partial\theta}) + \frac{\partial}{\partial\theta}(\frac{1}{R}N_{\theta 0}\frac{\partial w}{\partial\theta} + N_{x\theta 0}\frac{\partial w}{\partial x})\right] \quad\quad (18)$$

where stress resultants with subscript '0' denote the pre-buckling loads and they can be expressed for axial compression load as

$$N_{x0} = -\frac{P}{2\pi R(x)\cos\alpha} \qquad\qquad N_{\theta 0} = 0 \qquad\quad N_{x\theta 0} = 0 \tag{19}$$

The boundary conditions are then given by

$$\int_{\Gamma} \left[(RN_x - R\hat{N}_x)\delta u - (RN_{x\theta} - M_{x\theta}\cos\alpha - R\hat{T}_x)\delta v \right.$$
$$+ (RM_x - R\hat{M}_x)\delta(\frac{\partial w}{\partial x}) + (RN_x\frac{\partial w}{\partial x} + \frac{\partial(RM_x)}{\partial x} \tag{20}$$
$$\left. -M_{\theta}\sin\alpha + 2\frac{\partial M_{x\theta}}{\partial\theta} + N_{x\theta}\frac{\partial w}{\partial\theta} - R\hat{V}_x)\delta w \right]d\theta = 0$$

Thus -neglecting nonlinear terms- the primary or essential variables *(i.e.,* generalized displacements) are u_0, v_0, w_0, $\partial w_0/\partial x$ and secondary variables (i.e., generalized forces) are N_x, T_x, V_x, M_x in which

$$V_x = Q_x + \frac{1}{R}\frac{\partial M_{x\theta}}{\partial\theta}$$
$$\tag{21}$$
$$T_x = N_{x\theta} + \frac{M_{x\theta}}{R}\cos\alpha$$

3. Solutions for buckling of joined laminated conical shells

By the use of trigonometric solution in θ direction

$$u(x,\theta) = u(x)\cos n\theta$$
$$v(x,\theta) = v(x)\sin n\theta \tag{22}$$
$$w(x,\theta) = w(x)\cos n\theta$$

and series solution in *x* direction, and with the approach described by Tong and Wang (1992) we have

$$u(x) = \sum_{m=0}^{\infty} a_m x^m$$
$$v(x) = \sum_{m=0}^{\infty} b_m x^m \tag{23}$$
$$w(x) = \sum_{m=0}^{\infty} c_m x^m$$

where a_m, b_m and c_m are constants which can be determined by recurrence relations obtained by substitution of Eqs. (22) and (23) into Eq. (16) and matching the terms of same order in *x*. After some manipulation we have

$$a_{m+2} = G_{1,1}a_{m+1} + G_{1,2}a_m + G_{1,3}a_{m-1} + G_{1,4}b_{m+1} + G_{1,5}b_m + G_{1,6}b_{m-1}$$
$$+ G_{1,7}c_{m+3} + G_{1,8}c_{m+2} + G_{1,9}c_{m+1} + G_{1,10}c_m + G_{1,11}c_{m-1}$$

$$b_{m+2} = G_{2,1}a_{m+1} + G_{2,2}a_m + G_{2,3}a_{m-1} + G_{2,4}a_{m-2}$$
$$+ G_{2,5}b_{m+1} + G_{2,6}b_m + G_{2,7}b_{m-1} + G_{2,8}b_{m-2}$$
$$+ G_{2,9}c_{m+2} + G_{2,10}c_{m+1} + G_{2,11}c_m + G_{2,12}c_{m-1} + G_{2,13}c_{m-2} \tag{24}$$

$$c_{m+4} = G_{3,1}a_{m+2} + G_{3,2}a_{m+1} + G_{3,3}a_m + G_{3,4}a_{m-1}$$
$$+ G_{3,5}a_{m-2} + G_{3,6}b_{m+2} + G_{3,7}b_{m+1} + G_{3,8}b_m + G_{3,9}b_{m-1}$$
$$+ G_{3,10}b_{m-2} + G_{3,11}c_{m+3} + G_{3,12}c_{m+2} + G_{3,13}c_{m+1}$$
$$+ G_{3,14}c_m + G_{3,15}c_{m-1} + G_{3,16}c_{m-2}$$

$G_{i,j}$ coefficients are given in the Appendix. With these equations, one can evaluate all coefficients in $u(x)$, $v(x)$ and $w(x)$. Coefficients a_0, a_1, b_0, b_1, c_0, c_1, c_2 and c_3 should be calculated from the boundary and continuity conditions. The general form of displacement functions $u(x)$, $v(x)$ and $w(x)$ are in the form

$$u(x) = u_1(x)a_0 + u_2(x)a_1 + u_3(x)b_0 + u_4(x)b_1 + u_5(x)c_0 + u_6(x)c_1 + u_7(x)c_2 + u_8(x)c_3$$
$$v(x) = v_1(x)a_0 + v_2(x)a_1 + v_3(x)b_0 + v_4(x)b_1 + v_5(x)c_0 + v_6(x)c_1 + v_7(x)c_2 + v_8(x)c_3 \tag{25}$$
$$w(x) = w_1(x)a_0 + w_2(x)a_1 + w_3(x)b_0 + w_4(x)b_1 + w_5(x)c_0 + w_6(x)c_1 + w_7(x)c_2 + w_8(x)c_3$$

3.1 Boundary and continuity conditions

All boundary conditions can be used at both ends of the joined cones. We use four subclasses of simply-supported, clamped and free boundary conditions as

$$\begin{aligned} &\text{S1:} && N_{x\theta} = N_x = M_x = w = 0 \\ &\text{S2:} && N_{x\theta} = u = M_x = w = 0 \\ &\text{S3:} && v = N_x = M_x = w = 0 \\ &\text{S4:} && v = u = M_x = w = 0 \end{aligned} \tag{26}$$

$$\begin{aligned} &\text{C1:} && N_{x\theta} = N_x = \partial w / \partial x = w = 0 \\ &\text{C2:} && N_{x\theta} = u = \partial w / \partial x = w = 0 \\ &\text{C3:} && v = N_x = \partial w / \partial x = w = 0 \\ &\text{C4:} && v = u = \partial w / \partial x = w = 0 \end{aligned} \tag{27}$$

$$\begin{aligned}
\text{F1:} \quad & N_{x\theta} = N_x = M_x = Q_x = 0 \\
\text{F2:} \quad & N_{x\theta} = u = M_x = Q_x = 0 \\
\text{F3:} \quad & v = N_x = M_x = Q_x = 0 \\
\text{F4:} \quad & v = u = M_x = Q_x = 0
\end{aligned} \tag{28}$$

All of the above mentioned boundary conditions are applicable in the current solution method. The continuity conditions at the conical shell joint can be obtained from Eq. (20) as:

$$\begin{aligned}
& u_1 \cos \alpha_1 - w_1 \sin \alpha_1 = u_2 \cos \alpha_2 - w_2 \sin \alpha_2 \\
& u_1 \sin \alpha_1 + w_1 \cos \alpha_1 = u_2 \sin \alpha_2 + w_2 \cos \alpha_2 \\
& v_1 = v_2 \\
& \frac{\partial w_1}{\partial x_1} = \frac{\partial w_2}{\partial x_2} \\
& N_{x1} \cos \alpha_1 - V_{x1} \sin \alpha_1 = N_{x2} \cos \alpha_2 - V_{x2} \sin \alpha_2 \\
& N_{x1} \sin \alpha_1 + V_{x1} \cos \alpha_1 = N_{x2} \sin \alpha_2 + V_{x2} \cos \alpha_2 \\
& T_{x1} = T_{x2} \\
& M_{x1} = M_{x2}
\end{aligned} \tag{29}$$

Applying Eqs. (22) and (23) in continuity conditions and desired boundary conditions results in a set of 16 algebraic equations as eigenvalue problem and the axial buckling load of the joined cross-ply conical shells can be obtained by solving this eigenvalue problem.

4. Numerical results and discussions

4.1 Comparative study

To validate the results, we assume that two conical shells have the same lengths, thicknesses and semi-vertex angles so that we can compare the results with the available results in the literature for a single conical shell. All the results of present study are extracted using 30 terms of series solution. The values of buckling ratio ρ_{cr} and circumferential wave number n obtained from the present study along with results presented in (Tong and Wang 1992) are shown in Table 1. The buckling ratio ρ_{cr} is defined as

$$\rho_{cr} = \frac{P_{cr}}{P_{cyl}} \tag{30}$$

where P_{cr} is the buckling load obtained, and P_{cyl} is the classical value of the buckling load for a long cylindrical shell with simply supported boundary conditions

$$P_{cyl} = \frac{2\pi E_1 t^2}{\sqrt{3(1 - v_{12}{}^2)}} \tag{31}$$

The coefficients in the constitutive Eq. (6) for anti-symmetric cross-ply laminate is (Tong and Wang 1992)

$$A_{11} = A_{22} = \frac{1}{2}(Q_{11} + Q_{22})t, \qquad A_{12} = Q_{12}t, \qquad A_{66} = Q_{66}t$$

$$B_{11} = -B_{22} = \pm\frac{1}{4N_L}(Q_{11} - Q_{22})t^2, \qquad B_{12} = 0, \qquad B_{66} = 0 \qquad (32)$$

$$D_{11} = D_{22} = \frac{1}{24}(Q_{11} + Q_{22})t^3, \qquad D_{12} = \frac{1}{12}Q_{12}t^3, \qquad D_{66} = \frac{1}{12}Q_{66}t^3$$

The material of lamina is assumed to be graphite/epoxy, with the following properties (Tong and Wang 1992):

$$\frac{E_1}{E_2} = 40.0, \qquad \frac{G_{12}}{E_2} = 0.5$$
$$\nu_{12} = 0.25, \qquad E_2 = 10\,\text{GPa} \qquad (33)$$

The results are shown in Table 1 for different values of L/R_0 and semi-vertex angles (α). Good agreement for ρ_{cr} can be observed.

In addition, Table 2 presents the comparison of the results of this study with finite element method (FEM) for cross-ply laminated conical shells with various stacking sequences in which $R_1/h = 100$, $L/R_1 = 0.2$ and $\alpha = 30°$.

The FE analysis is performed using ANSYS software with 4-node shell element with linear element formulation, reduced-integration, and hour-glass control, which has six degrees of freedom at each node, three translational displacements in the nodal directions and three rotational displacements about the nodal axes. The boundary condition is considered to be S4 simply-supported at both ends. The model subjected to axial compression and the mesh convergence is obtained using 800 elements. By the use of LANCZOS method, (Moaveni 2015) eigenvalue problem is solved and the linear buckling load for various stacking sequences is investigated. Results are in good accordance both in critical load ratio and circumferential wave numbers.

Table 1 Buckling ratio ρ_{cr} and circumferential wave number(n) for anti-symmetric cross-ply laminate with S4 boundary conditions ($R_1/h = 100.0$)

L/R_0	N_L	$\alpha = 10°$		$\alpha = 30°$	
		Present	Tong and Wang (1992)	Present	Tong and Wang (1992)
0.2	2	0.1621(9)	0.1615(9)	0.1392(9)	0.1370(9)
	4	0.2160(8)	0.2151(8)	0.1862(8)	0.1832(8)
	6	0.2200(8)	0.2190(8)	0.1897(8)	0.1867(8)
	∞	0.2211(8)	0.2202(8)	0.1911(8)	0.1878(7)
0.5	2	0.0768(9)	0.0769(9)	0.0626(7)	0.0629(9)
	4	0.1060(6)	0.1068(6)	0.0829(6)	0.0830(6)
	6	0.1076(6)	0.1085(6)	0.0842(6)	0.0846(6)
	∞	0.1072(6)	0.1081(6)	0.0840(6)	0.0845(6)

Table 2 Buckling ratio ρ_{cr} and circumferential wave number(n) for various stacking sequences for S4 boundary conditions ($R_1/h = 100.0$, $L/R_1 = 0.2$ and $\alpha = 30°$)

Stacking sequences	Present	FE
(0/0/90)	0.1094(8)	0.1091(8)
(0/90/90)	0.1652(9)	0.1616(8)
(0/90/0)	0.0589(7)	0.0578(7)
(0/90/90/90)	0.1860(10)	0.1747(8)
(0/0/90/90)	0.1343(9)	0.1319(8)
(0/0/90/0)	0.0620(7)	0.0603(7)
(0/90)$_S$	0.0841(7)	0.0815(7)
(0$_2$/90)$_S$	0.0589(7)	0.0578(7)
(0/90/0)$_S$	0.1247(7)	0.1183(7)
(0/90$_2$)$_S$	0.1336(7)	0.1255(7)

NL = 2   *NL* = 4

NL = 6   *NL* = ∞
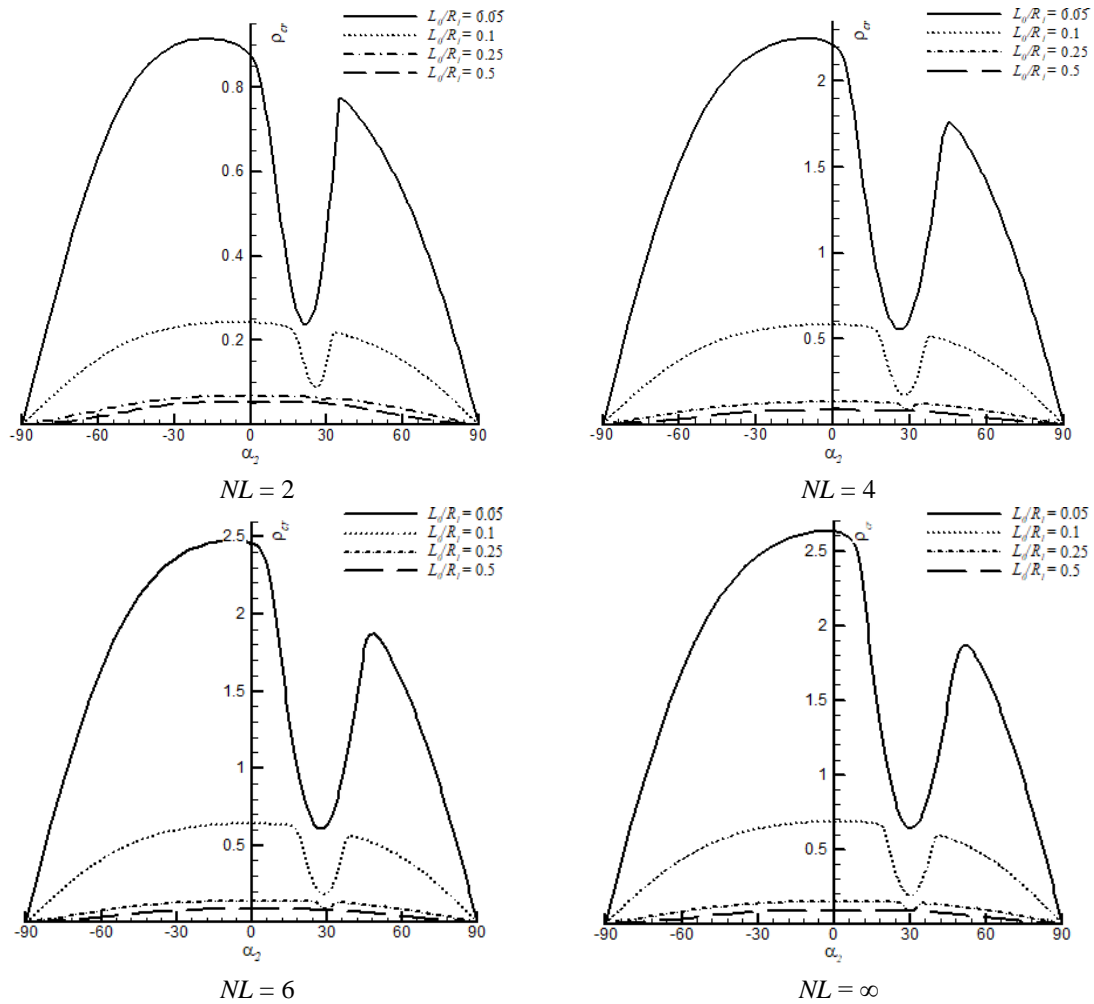
Fig. 3 Effects of L/R_1 on the buckling ratio of joined conical shells versus α_2 for various numbers of layers [α_1=30°]
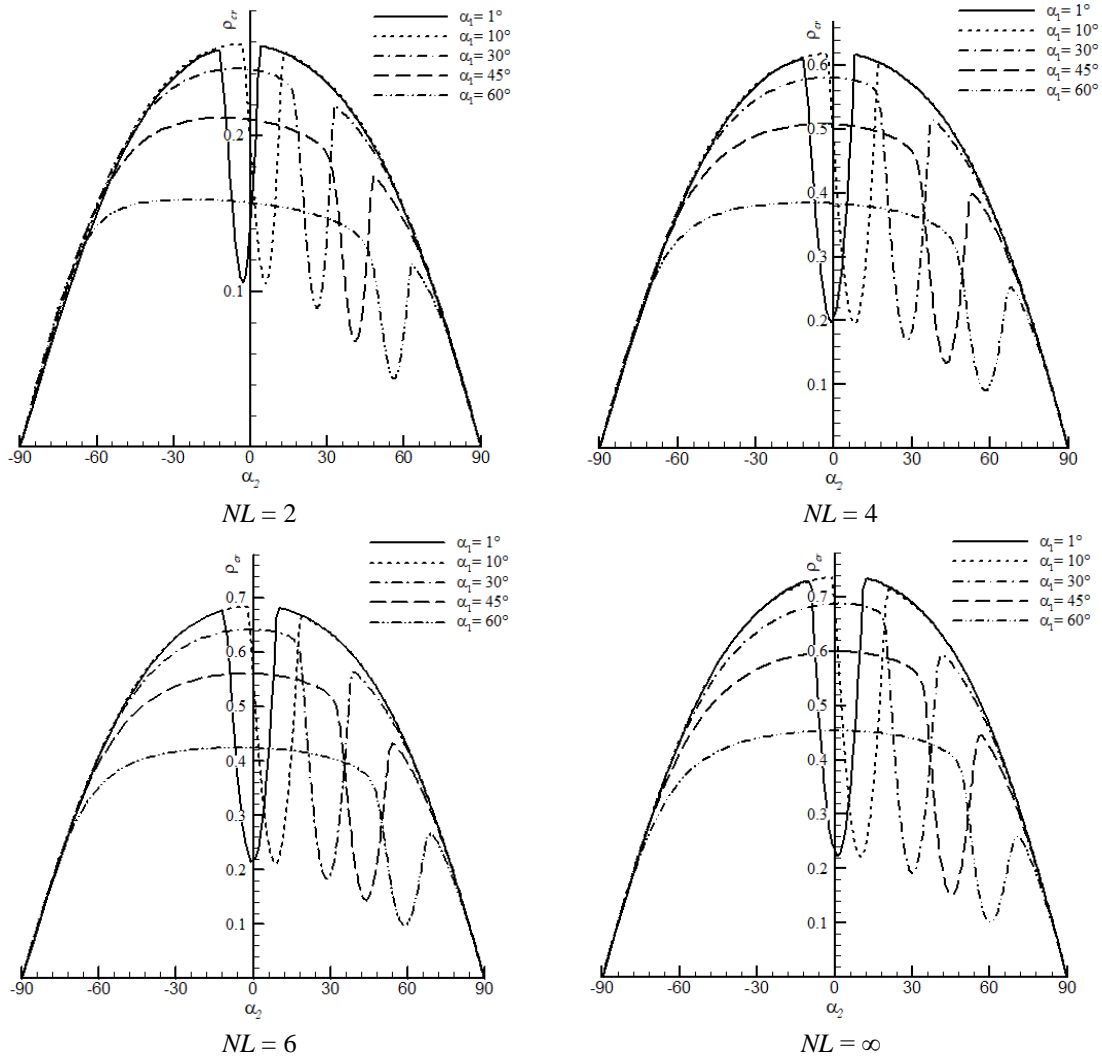
Fig. 4 Variation of buckling ratio for different values of N_L and α_1 [$L_0/R_1 = 0.1$ and $R_1/h = 100.0$]

4.2 Results

In this section we use the above formulation to study the buckling load of joined anti-symmetric cross-ply conical shells. For simplicity, we assume that the shells are made from one material and all mechanical properties and also the lengths and thicknesses are the same. Thus we have:

$$E_1 = E_2 , \quad v_1 = v_2 , \quad L_1 = L_2 = L_0 , \quad t_1 = t_2 \tag{34}$$

The effect of L_0/R_1 on the buckling load of joined conical shells versus α_2 for various numbers of layers is shown in Fig. 3. In this figure α_1 is set to 30^0. It is seen that the buckling load of joined shells increase when α_2 moves towards zero (*i.e.* joined cone-cylinder shells). However, for small values of L_0/R_1, the buckling load drops rapidly when α_2 is close to α_1.
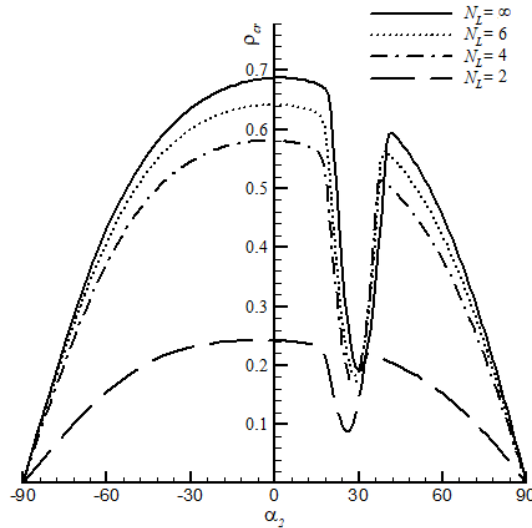
Fig. 5 Variation of buckling ratio for different values of N_L [$L_0/R_1 = 0.1$, $\alpha_1 = 30^o$ and $R_1/h = 100.0$]
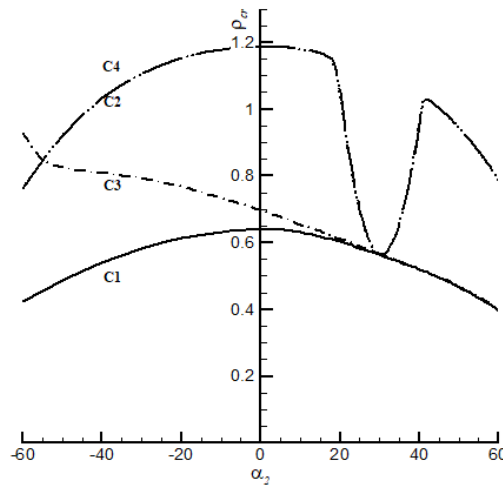
Fig. 6 Variation of buckling ratio for different types of clamped boundary conditions [$L_0/R_1 = 0.1$, $\alpha_1 = 30^o$ and $N_L = 6$]

Fig. 4 shows the buckling ratio for $L_0/R_1 = 0.1$ and different values of N_L and α_1. It can be seen from Fig. 3 and 4 that the minimum value of buckling load with specified lengths occurs when α_2 is close to α_1 but it varies by number of layers.

Effect of number of layers on buckling ratio of joined anti-symmetric cross-ply conical shells is shown in Fig. 5. It is assumed that $L_0/R_1 = 0.1$ and $\alpha_1 = 30^o$. It is seen that the buckling load of joined shells is very low when we have only 2 layers. It is due to the effect of strong asymmetry of lamination sequence that causes buckling in lower loads. When we use more layers, the laminate approach to symmetric condition and the buckling load get larger. In addition, the place of minimum buckling ratio (i.e., the α_2) varies with number of layers from angles 3 degrees less to 3 degrees more than α_1.

Effect of various types of clamped boundary conditions at both ends on buckling loads of joined anti-symmetric cross-ply conical shells is shown in Fig. 6. It is assumed that $L_0/R_1 = 0.1$, $\alpha_1 = 30^o$ and $N_L = 6$. It can be seen that when $\alpha_1 = \alpha_2$, all four types of clamped boundary conditions have approximately the same buckling ratio and C2 and C4 types of clamped boundary conditions have the same behavior. However, when the semi-vertex angles are not the same, the change in buckling loads are dissimilar.

5. Conclusions

In this paper, the buckling load of two joined conical shells is studied and the results are validated with the other papers and finite element analysis. Meanwhile, the effects of semi-vertex angles, meridional lengths, number of layers and various kinds of simply supported and clamped boundary conditions at both ends on the buckling loads of joined anti-symmetric cross-ply conical shells is presented. The major outcomes of this study
• The buckling load of joined conical shells is increased when conical shells move towards the cylindrical shell.
• For the short cones, the buckling load of joined conical shells decreases rapidly when the two semi-vertex angles come close to each other. Usually, the minimum buckling load occurs when the semi-vertex angles are a few degrees apart from each other. The position of this minimum (on α_2 axis) varies with the number of layers.
• Using more layers (in constant thicknesses) of anti-symmetric laminates, the buckling load increase due to decrease in lamination sequence asymmetry of the conical shell.

References

Anwen, W. (1998), "Stresses and stability for the cone-cylinder shells with toroidal transition", *Int. J. Pres. Ves. Pip.*, **75**(1), 49-56. https://doi.org/10.1016/s0308-0161(98)00013-1.

Bagheri, H., Kiani, Y. and Eslami, M.R. (2018), "Free vibration of joined conical–cylindrical–conical shells", *Acta Mech.*, **229**(7), 2751-2764 https://doi.org/10.1007/s00707-018-2133-3.

Bushnell, D. and Galletly, G.D. (1974), "Comparisons of test and theory for nonsymmetric elastic-plastic buckling of shells of revolution", *Int. J. Solid Struct.*, **10**(11), 1271-1286.
https://doi.org/10.1016/0020-7683(74)90072-9.

Flores, F.G. and Godoy, L.A. (1991), "Post-buckling of elastic cone-cylinder and sphere-cylinder complex shells", *Int. J. Pres. Ves. Pip.*, **45**(2), 237-258. https://doi.org/10.1016/0308-0161(91)90095-j.

Izadi, M.H., Hosseini-Hashemi, S. and Korayem, M.H. (2018), "Analytical and FEM solutions for free vibration of joined cross-ply laminated thick conical shells using shear deformation theory", *Arch. Appl. Mech.*, **88**(12), 2231-2246. https://doi.org/10.1007/s00419-018-1446-y.

Kouchakzadeh, M.A. and Shakouri, M. (2014), "Free vibration analysis of joined cross-ply laminated conical shells", *Int. J. Mech. Sci.*, **78**, 118-125. https://doi.org/10.1016/j.ijmecsci.2013.11.008.

Kouchakzadeh, M. and Shakouri, M. (2015), "Analytical solution for axisymmetric buckling of joined conical shells under axial compression", *Struct. Eng. Mech.*, **54**(4), 649-664.
https://doi.org/10.12989/sem.2015.54.4.649.

Moaveni, S. (2015), *Finite Element Analysis: Theory and Application with ANSYS*, Pearson Education, India.

Patel, B.P., Shukla, K.K. and Nath, Y. (2005), "Thermal postbuckling analysis of laminated cross-ply truncated circular conical shells", *Compos. Struct.*, **71**(1), 101-114.
https://doi.org/10.1016/j.compstruct.2004.09.030.

Patel, B.P., Nath, Y. and Shukla, K.K. (2006), "Nonlinear thermo-elastic buckling characteristics of cross-ply laminated joined conical–cylindrical shells", *Int. J. Solid Struct.*, **43**(16), 4810-4829. https://doi.org/10.1016/j.ijsolstr.2005.07.025.

Patel, B.P., Singh, S. and Nath, Y. (2008), "Postbuckling characteristics of angle-ply laminated truncated circular conical shells", *Commun. Nonlinear Sci. Numer. Simul.*, **13**(7), 1411-1430. https://doi.org/10.1016/j.cnsns.2007.01.001.

Pietraszkiewicz, W. and Konopińska, V. (2015), "Junctions in shell structures: A review", *Thin Wall. Struct.*, **95**, 310-334. https://doi.org/10.1016/j.tws.2015.07.010.

Qatu, M.S. (2004), *Vibration of Laminated Shells and Plates*, Elsevier Science, U.K.

Reddy, J.N. (2004), *Mechanics of Laminated Composite Plates and Shells: Theory and Analysis*, CRC Press, Boca Raton, Florida, U.S.A.

Shakouri, M. and Kouchakzadeh, M.A. (2013), "Stability analysis of joined isotropic conical shells under axial compression", *Thin Wall. Struct.*, **72**, 20-27. http://doi.org/10.1016/j.tws.2013.06.012.

Shakouri, M. and Kouchakzadeh, M. (2014), "Free vibration analysis of joined conical shells: Analytical and experimental study", *Thin Wall. Struct.*, **85**, 350-358. https://doi.org/10.1016/j.tws.2014.08.022.

Shakouri, M., Spagnoli, A. and Kouchakzadeh, M. (2016), "Effects of imperfection shapes on buckling of conical shells under compression" *Struct. Eng. Mech.*, **60**(3), 365-386. https://doi.org/10.12989/sem.2016.60.3.365.

Sarkheil, S., Saadat Foumani, M. and Navazi, H.M. (2017), "Free vibrations of a rotating shell made of p joined cones", *Int. J. Mech. Sci.*, **124**, 83-94. https://doi.org/10.1016/j.ijmecsci.2017.02.003.

Teng, J.G. (1996), "Elastic buckling of cone-cylinder intersection under localized circumferential compression", *Eng. Struct.*, **18**(1), 41-48. https://doi.org/10.1016/0141-0296(95)00114-3.

Teng, J.G. and Barbagallo, M. (1997), "Shell restraint to ring buckling at cone-cylinder intersections", *Eng. Struct.*, **19**(6), 425-431. https://doi.org/10.1016/s0141-0296(96)00087-9.

Teng, J.G. and Ma, H.-W. (1999), "Elastic buckling of ring-stiffened cone–cylinder intersections under internal pressure", *Int. J. Mech. Sci.*, **41**(11), 1357-1383. https://doi.org/10.1016/s0020-7403(98)00097-6.

Tong, L. and Wang, T.K. (1992), "Simple solutions for buckling of laminated conical shells", *Int. J. Mech. Sci.*, **34**(2), 93-111. https://doi.org/10.1016/0020-7403(92)90076-s.

Zerin, Z. (2012), "The effect of non-homogeneity on the stability of laminated orthotropic conical shells subjected to hydrostatic pressure", *Struct. Eng. Mech.*, **43**(1), 89-103. https://doi.org/10.12989/sem.2012.43.1.089.

Zhao, Y. and Teng, J.G. (2003), "A stability design proposal for cone–cylinder intersections under internal pressure", *Int. J. Pres. Ves. Pip.*, **80**(5), 297-309. https://doi.org/10.1016/s0308-0161(03)00048-6.

CC

Appendix

$$G_{1,1}(m) = -\frac{(3m+1)\sin\alpha}{(m+2)R_0}$$

$$G_{1,2}(m) = \frac{\sin^2\alpha(A_{11}(1-3m)m+A_{22})+A_{66}n^2}{A_{11}(m+1)(m+2)R_0^2}$$

$$G_{1,3}(m) = \frac{\sin^3\alpha(A_{22}-A_{11}(m-1)^2)+A_{66}n^2\sin\alpha}{A_{11}(m+1)(m+2)R_0^3}$$

$$G_{1,4}(m) = -\frac{n((A_{12}+A_{66})R_0+(B_{12}+B_{66})\cos\alpha)}{A_{11}(m+2)R_0^2}$$

$$G_{1,5}(m) = \frac{n\sin\alpha(R_0(-2(A_{12}+A_{66})m+A_{22}+A_{66})+\cos\alpha(B_{12}(-(m-1))-B_{66}(m-2)+B_{22}))}{A_{11}(m+1)(m+2)R_0^3}$$

$$G_{1,6}(m) = \frac{n\sin^2\alpha(A_{12}(-(m-1))-A_{66}(m-2)+A_{22})}{A_{11}(m+1)(m+2)R_0^3}$$

$$G_{1,7}(m) = \frac{B_{11}(m+3)}{A_{11}}$$

$$G_{1,8}(m) = \frac{B_{11}(3m+1)\sin\alpha}{A_{11}R_0}$$

$$G_{1,9}(m) = \frac{-A_{12}R_0\cos\alpha+\sin^2\alpha(B_{11}m(3m-1)-B_{22})-(B_{12}+2B_{66})n^2}{A_{11}(m+2)R_0^2}$$

$$G_{1,10}(m) = (\sin\alpha(2R_0\cos\alpha(A_{22}-2A_{12}m)+2B_{11}(m-1)^2m\sin^2\alpha+B_{22}m\cos 2\alpha$$
$$-2B_{12}(m-1)n^2-4B_{66}mn^2-B_{22}m+2B_{22}n^2+4B_{66}n^2))/(2A_{11}(m+1)(m+2)R_0^3)$$

$$G_{1,11}(m) = \frac{\sin^2\alpha\cos\alpha(A_{22}-A_{12}(m-1))}{A_{11}(m+1)(m+2)R_0^3}$$

$$G_{2,1}(m) = \frac{(A_{12}+A_{66})nR_0+(B_{12}+B_{66})n\cos\alpha}{(m+2)(R_0(A_{66}R_0+2B_{66}\cos\alpha)+D_{66}\cos^2\alpha)}$$

$$G_{2,2}(m) = \frac{n\sin\alpha(R_0(3(A_{12}+A_{66})m+A_{22}+A_{66})+\cos\alpha(2(B_{12}+B_{66})m+B_{22}+B_{66}))}{(m+1)(m+2)R_0(R_0(A_{66}R_0+2B_{66}\cos\alpha)+D_{66}\cos^2\alpha)}$$

$$G_{2,3}(m) = \frac{n\sin^2\alpha(R_0(3A_{12}(m-1)+A_{66}(3m-1)+2A_{22})+\cos\alpha(B_{12}(m-1)+B_{66}m+B_{22}))}{(m+1)(m+2)R_0^2(R_0(A_{66}R_0+2B_{66}\cos\alpha)+D_{66}\cos^2\alpha)}$$

$$G_{2,4}(m) = \frac{n\sin^3\alpha(A_{12}(m-2)+A_{66}(m-1)+A_{22})}{(m+1)(m+2)R_0^2(R_0(A_{66}R_0+2B_{66}\cos\alpha)+D_{66}\cos^2\alpha)}$$

$$G_{2,1}(m) = \frac{(A_{12} + A_{66})nR_0 + (B_{12} + B_{66})n\cos\alpha}{(m+2)(R_0(A_{66}R_0 + 2B_{66}\cos\alpha) + D_{66}\cos^2\alpha)}$$

$$G_{2,2}(m) = \frac{n\sin\alpha(R_0(3(A_{12} + A_{66})m + A_{22} + A_{66}) + \cos\alpha(2(B_{12} + B_{66})m + B_{22} + B_{66}))}{(m+1)(m+2)R_0(R_0(A_{66}R_0 + 2B_{66}\cos\alpha) + D_{66}\cos^2\alpha)}$$

$$G_{2,3}(m) = \frac{n\sin^2\alpha(R_0(3A_{12}(m-1) + A_{66}(3m-1) + 2A_{22}) + \cos\alpha(B_{12}(m-1) + B_{66}m + B_{22}))}{(m+1)(m+2)R_0^2(R_0(A_{66}R_0 + 2B_{66}\cos\alpha) + D_{66}\cos^2\alpha)}$$

$$G_{2,4}(m) = \frac{n\sin^3\alpha(A_{12}(m-2) + A_{66}(m-1) + A_{22})}{(m+1)(m+2)R_0^2(R_0(A_{66}R_0 + 2B_{66}\cos\alpha) + D_{66}\cos^2\alpha)}$$

$$G_{2,5}(m) = -\frac{\sin\alpha(R_0(A_{66}(4m+1)R_0 + 6B_{66}m\cos\alpha) + D_{66}(2m-1)\cos^2\alpha)}{(m+2)R_0(R_0(A_{66}R_0 + 2B_{66}\cos\alpha) + D_{66}\cos^2\alpha)}$$

$$G_{2,6}(m) = (4R_0(\sin^2\alpha(A_{66}(-6m^2 + 3m + 1)R_0$$
$$+ B_{66}(1 - 6(m-1)m)\cos\alpha) + A_{22}n^2R_0 + 2B_{22}n^2\cos\alpha) - D_{66}(m-2)m\sin^2 2\alpha$$
$$+ 4D_{22}n^2\cos^2\alpha) / (4(m+1)(m+2)R_0^2(R_0(A_{66}R_0 + 2B_{66}\cos\alpha) + D_{66}\cos^2\alpha))$$

$$G_{2,7}(m) = \frac{\sin\alpha(\sin^2\alpha(A_{66}((9-4m)m - 3)R_0 + B_{66}(-2(m-3)m - 3)\cos\alpha) + 2A_{22}n^2R_0 + 2B_{22}n^2\cos\alpha)}{(m+1)(m+2)R_0^2(R_0(A_{66}R_0 + 2B_{66}\cos\alpha) + D_{66}\cos^2\alpha)}$$

$$G_{2,8}(m) = \frac{A_{22}n^2\sin^2\alpha - A_{66}(m-3)(m-1)\sin^4\alpha}{(m+1)(m+2)R_0^2(R_0(A_{66}R_0 + 2B_{66}\cos\alpha) + D_{66}\cos^2\alpha)}$$

$$G_{2,9}(m) = -\frac{n((B_{12} + 2B_{66})R_0 + (D_{12} + 2D_{66})\cos\alpha)}{R_0(A_{66}R_0 + 2B_{66}\cos\alpha) + D_{66}\cos^2\alpha}$$

$$G_{2,10}(m) = -\frac{n\sin\alpha(R_0(3B_{12}m + 6B_{66}m + B_{22}) + \cos\alpha(2D_{12}m + 4D_{66}m + D_{22}))}{(m+2)R_0(R_0(A_{66}R_0 + 2B_{66}\cos\alpha) + D_{66}\cos^2\alpha)}$$

$$G_{2,11}(m) = (n(\cos\alpha(4A_{22}R_0^2 - m(D_{12}(m-1) + 2D_{66}(m-1) + D_{22}) + 4D_{22}n^2)$$
$$+ 2R_0(B_{22}(-2m + 2n^2 + 1) - 3(B_{12} + 2B_{66})(m-1)m)$$
$$+ 2R_0\cos 2\alpha(2B_{22}m + 3(B_{12} + 2B_{66})(m-1)m + B_{22})$$
$$+ m\cos 3\alpha(D_{12}(m-1) + 2D_{66}(m-1) + D_{22}))) / (4(m+1)(m+2)R_0^2(R_0(A_{66}R_0 + 2B_{66}\cos\alpha) + D_{66}\cos^2\alpha))$$

$$G_{2,12}(m) = (n(2A_{22}R_0\sin 2\alpha - 2B_{12}(m-2)(m-1)\sin^3\alpha - 4B_{66}(m-2)(m-1)\sin^3\alpha$$
$$+ B_{22}\sin\alpha(m\cos 2\alpha - m + 2n^2 + 2))) / (2(m+1)(m+2)R_0^2(R_0(A_{66}R_0 + 2B_{66}\cos\alpha) + D_{66}\cos^2\alpha))$$

$$G_{2,13}(m) = \frac{A_{22}n\sin\alpha\sin 2\alpha}{2(m+1)(m+2)R_0^2(A_{66}R_0^2 + 2B_{66}R_0\cos\alpha + D_{66}\cos^2\alpha)}$$

$$G_{3,1}(m) = \frac{A_{11}B_{11}(m-2)\sin\alpha}{(m+3)(m+4)R_0(A_{11}D_{11} - B_{11}^2)}$$

$$G_{3,2}(m) = (A_{11}(A_{12}R_0\cos\alpha + \sin^2\alpha(B_{11}((5-3m)m + 2) + B_{22}) + (B_{12} + 2B_{66})n^2)$$
$$- B_{11}(A_{22}\sin^2\alpha + A_{66}n^2)) / ((m+2)(m+3)(m+4)R_0^2(B_{11}^2 - A_{11}D_{11}))$$

$$G_{3,3}(m) = (\sin\alpha(A_{11}(2R_0\cos\alpha(3A_{12}m + A_{22}) - 2B_{11}(m-2)m(3m-1)\sin^2\alpha$$
$$+ B_{22}(1-2m)\cos 2\alpha + 4B_{12}mn^2 + 8B_{66}mn^2 + 2B_{22}(m+n^2) - B_{22})$$
$$- 2B_{11}(m+1)(A_{22}\sin^2\alpha + A_{66}n^2))) / (2m_{04}R_0^3(B_{11}^2 - A_{11}D_{11}))$$

$$G_{3,4}(m) = -(A_{11}\sin^2(\alpha)(2R_0\cos\alpha(3A_{12}(m-1) + 2A_{22}) + (m-2)\cos 2\alpha(B_{11}(m-1)^2 - B_{22})$$
$$+ 2n^2(B_{12}(m-1) + 2B_{66}(m-1) + B_{22}) - (m-2)(B_{11}(m-1)^2 - B_{22}))) / (2m_{04}R_0^4(A_{11}D_{11} - B_{11}^2))$$

$$G_{3,5}(m) = \frac{A_{11}\sin^3\alpha\cos\alpha(A_{12}(m-2) + A_{22})}{m_{04}R_0^4(B_{11}^2 - A_{11}D_{11})}$$

$$G_{3,6}(m) = (B_{11}n((A_{12} + A_{66})R_0 + (B_{12} + B_{66})\cos\alpha) - A_{11}n((B_{12} + 2B_{66})R_0$$
$$+ (D_{12} + 2D_{66})\cos\alpha)) / ((m+3)(m+4)R_0^2(B_{11}^2 - A_{11}D_{11}))$$

$$G_{3,7}(m) = (m+1)(n\sin\alpha(A_{11}(R_0(B_{22} - 3(B_{12} + 2B_{66})m) + \cos\alpha(-2D_{12}(m-1) - 4D_{66}(m-1) + D_{22}))$$
$$+ B_{11}(R_0(2A_{12}(m+1) + A_{66}(2m+1) - A_{22}) + \cos\alpha(B_{12}m + B_{66}(m-1) - B_{22})))) / (m_{04}R_0^3(B_{11}^2 - A_{11}D_{11}))$$

$$G_{3,9}(m) = (A_{11}n\sin\alpha(4A_{22}R_0\cos\alpha - 2B_{12}(m-2)(m-1)\sin^2\alpha - 4B_{66}(m-2)(m-1)\sin^2\alpha$$
$$+ B_{22}(-(m-3)\cos 2\alpha + m + 2n^2 - 1))) / (2m_{04}R_0^4(B_{11}^2 - A_{11}D_{11}))$$

$$G_{3,10}(m) = \frac{A_{11}A_{22}n\sin^2\alpha\cos\alpha}{m_{04}R_0^4(B_{11}^2 - A_{11}D_{11})}$$

$$G_{3,11}(m) = \frac{\sin\alpha(2A_{11}D_{11}(2m+1) - B_{11}^2(3m+4))}{(m+4)R_0(B_{11}^2 - A_{11}D_{11})}$$

$$G_{3,12}(m) = (A_{11}(R_0(P\sec\alpha - 4\pi B_{12}\cos\alpha) + 2\pi(\sin^2\alpha(6D_{11}m^2 - D_{22}) - 2(D_{12} + 2D_{66})n^2))$$
$$+ 2\pi B_{11}(A_{12}R_0\cos\alpha + B_{22}\sin^2\alpha + (B_{12} + 2B_{66})n^2)$$
$$- 2\pi B_{11}^2(m+1)(3m+2)\sin^2\alpha) / (2\pi(m+3)(m+4)R_0^2(B_{11}^2 - A_{11}D_{11}))$$

$$G_{3,13}(m) = (A_{11}(-6\pi B_{12}mR_0\sin 2\alpha + 2\pi(2m-1)\sin\alpha(\sin^2\alpha(2D_{11}(m-1)m - D_{22})$$
$$- 2(D_{12} + 2D_{66})n^2) + 3mPR_0\tan(\alpha)) + \pi B_{11}\sin\alpha(2R_0\cos\alpha(2A_{12}(m+1) - A_{22})$$
$$- B_{22}((m+1)\cos 2\alpha - m + 2n^2 - 1) + 2B_{12}mn^2 + 4B_{66}mn^2)$$
$$- 2\pi B_{11}^2m^2(m+1)\sin^3\alpha) / (2\pi(m+2)(m+3)(m+4)R_0^3(B_{11}^2 - A_{11}D_{11}))$$

$$G_{3,14}(m) = (A_{11} / (\pi(m+1)(-4\pi\cos 2\alpha(A_{22}R_0^2 + 4D_{66}(m-1)^2n^2 + D_{22}((m-2)m + 2n^2))$$
$$+ \pi(-4A_{22}R_0^2 + 16D_{66}(m-1)^2n^2 + D_{22}(3(m-2)m - 8n^4 + 8n^2)) +$$
$$+ 2R_0\cos\alpha(6(m-1)m(\pi B_{12} + P) + \pi B_{22}(1 - 8n^2)) - 2\pi R_0\cos 3\alpha(6B_{12}(m-1)m + B_{22})$$
$$- 8\pi D_{11}(m-2)(m-1)^2m\sin^4\alpha + \pi D_{22}(m-2)m\cos 4\alpha + 16\pi D_{12}(m-1)^2n^2\sin^2\alpha$$
$$- 12(m-1)mPR_0\sec\alpha + \frac{8B_{11}R_0\sin^2\alpha\cos\alpha(A_{22} - A_{12}m)}{A_{11}})) / (8(m+2)(m+3)(m+4)R_0^4(A_{11}D_{11} - B_{11}^2))$$

$$G_{3,15}(m) = (A_{11}\tan\alpha(\pi\cos^2\alpha(4A_{22}R_0\cos\alpha + B_{22}(\cos 2\alpha + 4n^2 - 1)) - \pi B_{12}(m-2)(m-1)\sin^2 2\alpha$$
$$+ (m-2)(m-1)P\sin^2(\alpha))) / (2\pi m_{04}R_0^4(B_{11}^2 - A_{11}D_{11}))$$

$$G_{3,16}(m) = \frac{A_{11}A_{22}\sin^2(\alpha)\cos^2(\alpha)}{m_{04}R_0^4(B_{11}^2 - A_{11}D_{11})}$$

$$m_{04} = (m+1)(m+2)(m+3)(m+4)$$